Machine Learning Methods for Rapid, Real-Time Pressure Readout from an Optics-Based Intraocular Pressure Sensor

Ashwin Balakrishna, Jeong Oen Lee, Hyuck Choo

ABSTRACT

Here, we discuss statistical methods for efficient and accurate pressure readout from a recently fabricated, optics-based intraocular pressure (IOP) sensor [1]. Optics-based IOP sensing methods using microscale implants are appealing as they allow for direct pressure measurements, making them more accurate than the indirect techniques used in most traditional measurement approaches. The sensor considered in this work is primarily composed of a reflective membrane, which when implanted into the eye, can be used to obtain high-resolution reflection spectra when focused light is shone into the center of the eye. However, conventional pressure extraction methods for such sensors are computationally expensive, making real-time pressure readout impractical. In this work, we design statistical methods to extract pressure measurements from sensor reflection spectra and demonstrate that these techniques achieve similar accuracy to the best traditional methods (within ± 1 mmHg) while improving on the computation time of these techniques by at least two orders of magnitude. These algorithms, combined with an optical sensing approach, can enable rapid, real-time, and accurate updates on a patient's IOP, and thus aid clinical treatment of diseases such as glaucoma, in which IOP is a critical diagnostic measure.

INTRODUCTION

Glaucoma is the primary cause of irreversible blindness, but can be treated by taking measures to control a patient's intraocular pressure (IOP) before their sight deteriorates past a critical point [2]. A detailed and accurate understanding of a patient's IOP profile can help physicians personalize treatments based on individualized trends, similar to the treatment methods used for other chronic progressive diseases such as hypertension and diabetes [3]. Traditional IOP measurement techniques only provide indirect pressure measurements, making their accuracy susceptible to corneal biomechanics differences. Thus, implantable IOP sensors are attractive as they provide direct IOP measurements, and thus enable high accuracy, regular IOP readout to monitor the health of patients at risk of chronic glaucoma [1].

Currently, an optics-based, hand-held detector has been developed in the Choo lab at Caltech to non-invasively measure intraocular pressure using a microscale, implantable sensor [1]. This sensor enables remote and accurate IOP readout that has successfully tracked artificially-induced, short-term transient IOP elevations in anesthetized rabbits [1]. The sensing mechanism consists of a reflective membrane, which when implanted into the eye, can be used to obtain high-resolution reflection spectra when focused near-infrared (NIR) light is shone into the center of a patient's eye [1]. These reflection spectra can be used to infer the degree of deflection of the sensor membrane using a standard Fabry-Perot optical cavity model, which can then be mapped to an ambient pressure reading using a solid mechanics model of the sensor membrane derived through its material properties. This method of combining the optical and mechanical properties of the sensing mechanism into an optomechanical model for pressure extraction is the standard method for determining IOP from optical signals [1]. However, this method is computationally expensive, making it impractical for use in real-time applications in which high time-resolution IOP signals are desirable for maximal clinical use.

This work improves on the previous pressure extraction methods by using statistical methods to extract IOP from the reflection spectra obtained from an optics-based IOP sensor. Our results closely match traditional physics-based models in terms of pressure extraction error while significantly outperforming them in terms of real-time evaluation speed. This has the potential to help make optics-based IOP sensing more commercially viable. Rapid and accurate pressure extraction algorithms, combined with an optics-based sensing approach, can enable patients to regularly measure IOP with a simple handheld device or smartphone, facilitating remote diagnosis by clinicians.

METHODS

Experimental Setup and Data

The optical spectra used for pressure extraction are collected using the experimental setup and sensor designed in [1]. Here, the sensor membrane is mounted in a controlled pressure chamber, in which the pressure can be precisely controlled between 0 and 40 mmHg using an open-tube manometer setup. This controlled pressure chamber is intended to be a representative model for the human eye, but one in which the ambient pressure, and thus simulated IOP, can be easily adjusted. Then, broadband NIR light from a tungsten bulb is shone into the center of the sensor membrane, with the resulting reflection spectra captured through a commercially

available spectrometer. A brief summary of the setup used is shown in Figure 1 below. These reflection spectra are then fed into a variety of different algorithms to map these signals to a specific IOP readout. An example reflection spectrum collected from the sensor is shown in Figure 2 below.

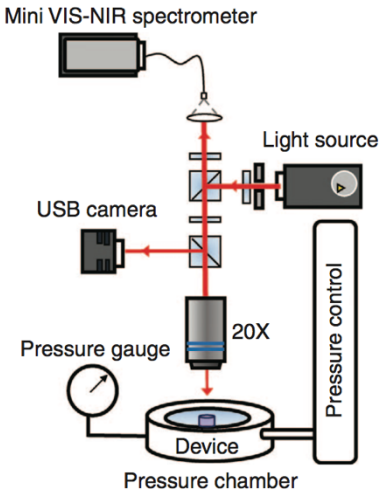

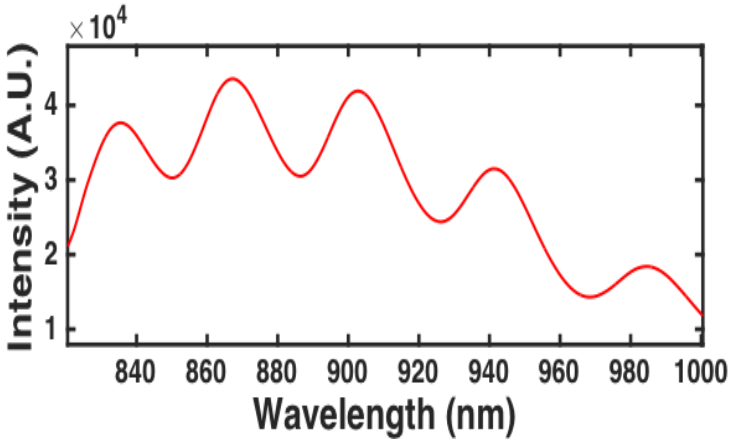

Figure 1 (left): *Schematic diagram of experimental setup*
Figure 2 (right): *Example reflection spectrum obtained from sensor at a given pressure after running it through a moving average filter.*

Using the experimental setup described, six datasets were collected of 15,000 optical spectra each, with each dataset consisting of spectra collected at a different ambient temperature between 30 and 37 degrees. Each collected spectra is paired with a reference pressure value, which can be used to evaluate the accuracy of any pressure extraction algorithm. These compiled datasets were used to test the various algorithms described in this work.

Feature Extraction

First, each collected reflection spectrum is run through a moving average filter for basic de-noising. Then, the two most prominent peak and two most prominent valley locations in wavelength space are found for each spectrum. Here, the prominence of each peak and valley is computed by determining how much each peak/valley stands out due to its intrinsic intensity and spacing relative to other peaks/valleys. Since the peak and valley locations were found to shift slightly in wavelength space at different pressures, the most prominent peak/valley locations were determined to be useful features we could extract from the collected reflection spectra. These features are identified in order to reduce the dimensionality of the pressure extraction

process while ensuring accurate results. Thus, each of the six initial datasets were converted to new datasets, in which just the four characteristic features of each spectrum (location of two most prominent peaks, location of two most prominent valleys) were stored along with the corresponding reference pressure value for that spectrum.

Pressure Extraction Algorithms

We compare five pressure extraction algorithms in terms of their real-time evaluation speed and accuracy on our collected datasets. All models were run on a MacBook Pro (Retina, 13-inch, Mid 2014, 2.6 GHz Intel Core i5 with 16GB of memory), and thus the computation times reported should be interpreted in this context. Each of these algorithms were designed to map the four most prominent peak/valley locations to a specific ambient pressure reading. Two of the algorithms discussed are physically-derived, while the other three are purely statistical, in which the function mapping peak/valley locations to a pressure value is essentially 'learned' through a parameterized model. All statistical models described below are trained on a randomly selected subset of the data consisting of 80% of the collected spectra (training set) and evaluated on the remaining 20% of the data (validation set).

<u>Physical Models</u>

I. Direct Mathematical Model: Here, a mechanical model of the sensor membrane that maps a specific ambient pressure to a membrane deflection [1], in addition to a theoretical mapping between the peak/valley locations of the optical reflection spectra and a given sensor membrane deflection [1] are used. When combined, these give a direct mapping between the peak/valley locations of each optical spectrum and the IOP.

II. Optomechanical (Conventional) Model: This is the most common way to map reflection spectra from physical membranes to a measure of membrane deflection, such as the ambient pressure of the membrane, which is the IOP for the sensor membrane discussed in this work [1]. Here, a mechanical model of the sensor membrane is used to map a specific ambient pressure to a membrane deflection [1]. Then, this membrane deflection is used to generate theoretical reflection spectra using a standard Fabry-Perot optical cavity model. The peak/valley locations in these theoretical spectra are then systematically matched with the peak/valley locations in the collected experimental spectra to extract a pressure value corresponding to any given experimental spectra. This optomechanical model is described in more detail in [1].

Statistical Methods

I. Fully Connected Neural Network (NN Model): A fully connected neural network is built using Keras, a wrapper around the Python TensorFlow library. The network designed has two layers, each with 8 hidden units, in addition to two 10% dropout layers. A mean squared error loss function is used along with the Adam optimizer and ReLU activation. All inputs to the model are normalized to have mean 0, standard deviation 1 for optimal performance, with the neural network output converted back to the original scale before it is reported.

II. Support Vector Machine (SVM Model): A support vector machine for regression was built using the Python scikit-learn library. A radial basis function kernel was used with a regularization penalty parameter of 0.5 and an epsilon tube of width 0.2.

III. Ensemble of Bagged Decision Trees (Tree-Based Model): A bagging regressor was implemented using the Python scikit-learn library. The base estimator used was a decision tree, while the maximum number of samples used to train each base estimator was set to be 70% of the total amount of training samples in the training set as a regularization measure. The number of estimators used in the ensemble was set to 100.

RESULTS

Now we compare the models described above in terms of their pressure extraction error. Pressure extraction error is measured in terms of the absolute value of the difference between each model's pressure output on a set of spectra and the reference pressure values for those spectra in the dataset. For all statistical models, the pressure extraction error is of course evaluated out of sample. Furthermore, all models are also compared based on their per-sample evaluation time in addition to the spread of their average pressure extraction errors over different temperatures. The spread of the pressure extraction residuals (predicted pressure – actual pressure) for each of the five methods are compared in Figure 3 below.

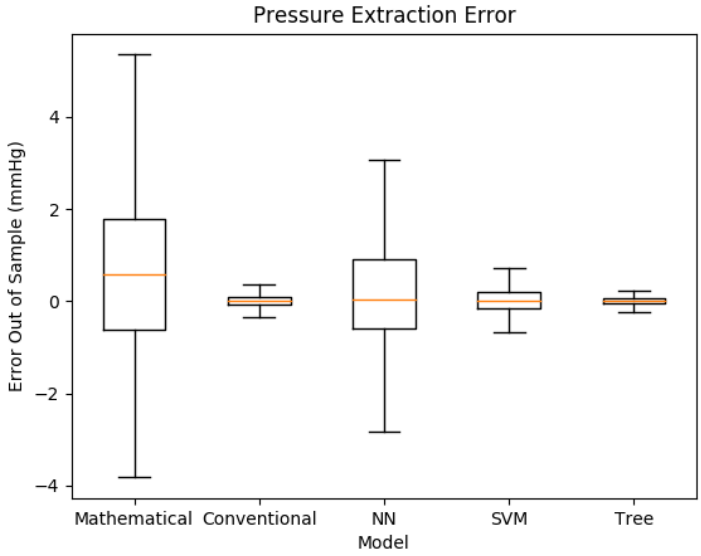

Figure 3: *Spread of the residuals of the computed pressure by each model and the reference pressure associated with each spectrum. Here, we see that the conventional model, SVM, and tree-based model all have very low errors in general, and are nearly always accurate to within* ± 1 *mmHg while the other models have much larger error spreads.*

Here, we see that the pressure extraction residuals for the direct mathematical model are actually very high, which may indicate that the theoretical mapping it uses does not handle the degree of noise in the collected data very well. Thus, we observe a spread of errors of nearly ± 2 mmHg. However, the error spread of the other models is relatively lower, especially the SVM, conventional model, and tree-based model. Interestingly, the spread of errors for the tree-based model is actually lower than that of either of the physics-based models, indicating that statistical models can actually outperform deterministic models from an accuracy standpoint in this application.

The spread of the per-sample evaluation time for each of the methods is compared in Figure 4 below.

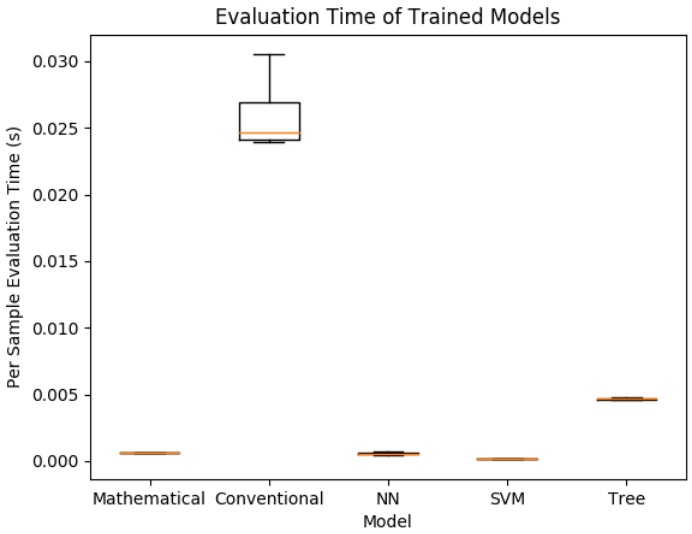

Figure 4: *Spread of the per-sample evaluation time of each model. Here, we see that the conventional model has a very high per-sample evaluation time, with a great degree of variation between different spectra. However, the per-sample evaluation time for the other models has very little variation, and the mathematical model, SVM, and NN Model have particularly low per-sample evaluation times.*

We see that the per-sample evaluation time and its spread are significantly higher for the conventional model than for any of the other models. This makes sense since the process of matching the experimental peak/valley locations to theoretical spectra is quite computationally expensive. Furthermore, the tree-based model has the next highest per-sample evaluation time, which makes sense since this model involves training an ensemble of 100 decision trees. The other models, however, have very low per-sample evaluation time (on the order of a few 100 microseconds), making them well-suited for real-time pressure readout applications.

Finally, the spread of the average pressure extraction error of each method over different temperatures is compared in Figure 5 below.

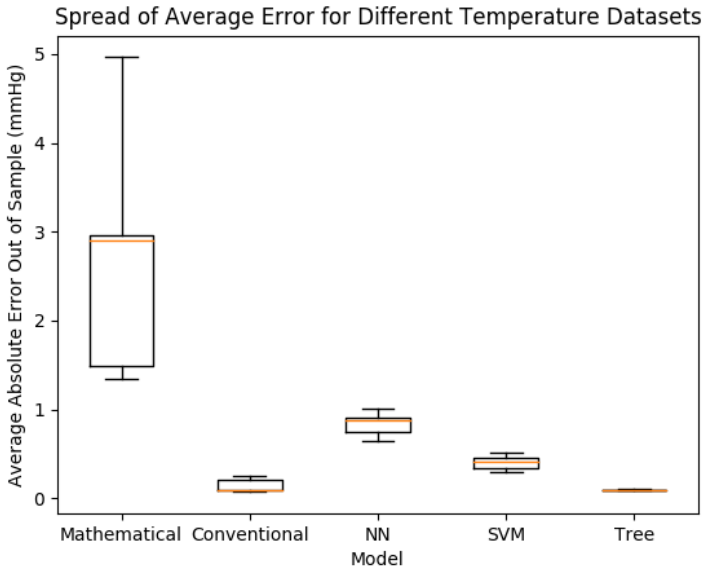

Figure 5: *Average pressure extraction error is computed for each model on each of the 6 temperature datasets. Then, the spread of the average pressure extraction error is shown for each model over the 6 different temperatures.*

We see that the mathematical model is very susceptible to temperature variation as the spread of the average pressure extraction error on different temperature datasets is much higher for the mathematical model than for the other models. Particularly, the tree-based model has very low variation in performance for different temperatures, indicating that it is particularly robust compared to the other models.

Ultimately, from the comparison performed above, we see that the SVM model has the lowest per-sample evaluation time, low pressure extraction error, and is robust to temperature changes making it the best model to use for real-time pressure readout applications. However, the tree-based model is also attractive if one is willing to sacrifice some time-resolution in the readout process, as although it is substantially slower than the SVM model, it is also the most accurate model explored in this work and the most robust to temperature changes. It is interesting to note that the most successful models were the statistical ones. Of the two physically-derived models, the mathematical model has very high error and low computation time, while the conventional model has relatively low error but very high computation time.

DISCUSSION

This work presents statistical methods that enable rapid and accurate pressure readout from a recently fabricated, optics-based, intraocular pressure (IOP) sensor. These methods are shown to improve the computation time of the pressure readout process while achieving similar pressure extraction error to existing, physics-based methods. Particularly, a 2-layer fully connected neural network, an ensemble of bagged decision trees (tree-based model), and an SVM are compared to standard optomechanical and direct mathematical models in terms of both accuracy and computation time. It is found that the ensemble of bagged decision trees, SVM, and optomechanical models all achieve sufficiently low out of sample error (less than ± 1 mmHg). Furthermore, the evaluation time of the SVM model is typically around 100 μs, making this model particularly attractive for use in a real-time pressure readout application since it outperforms all other tested models in terms of computation time, and has only slightly higher average absolute out of sample error (0.4 mmHg) compared to the tree-based (0.09 mmHg) and optomechanical (0.12 mmHg) models.

Furthermore, we also investigate how robust the five algorithms studied are to changes in the ambient temperature of the eye. It is found that the tree-based model is the least affected by data collected at different temperatures, with nearly no deviation in the average pressure extraction error for different temperature datasets. The SVM model is close behind in this regard, and both the SVM and tree-based models have smaller average error spread for different temperature datasets than either of the physically-derived models. Thus, the SVM and tree-based models achieve comparable readout accuracy to the best physically-derived method investigated here (the tree-based model's accuracy was actually better) while having significantly lower computation time and lower variation in performance with respect to ambient temperature.

We demonstrate that real-time, accurate IOP readout systems can significantly benefit from statistical methods from both an accuracy and speed standpoint. The evaluation time improvement afforded by these methods enables acquisition of high-resolution IOP signals from patients, improving a doctor's ability to effectively diagnose patients with diseases such as glaucoma, in which IOP is the primary adjustable risk factor. Future work could involve further tuning model parameters to improve results, trying different model architectures, or studying ways to infer further clinical information from the sensor reflection spectra beyond just IOP.

REFERENCES

[1] Jeong Oen Lee, Haeri Park, Juan Du, Ashwin Balakrishna, Oliver Chen, David Stretavan, Hyuck Choo. A Microscale Optical Implant for Continuous In-vivo Monitoring of Intraocular Pressure. *Microsystems & Nanoengineering* 2017.

[2] Quigley HA, Broman AT. The number of people with glaucoma worldwide in 2010 and 2020. *The British Journal of Ophthalmology* 2006; 90: 262–267.

[3] Hughes E, Spry P, Diamond J. 24-hour monitoring of intraocular pressure in glaucoma management: A retrospective review. *Journal of glaucoma* 2003; 12: 232–236.